Moment of inertia and rotational instability of gluon plasma

A. A. Roenko[1],

in collaboration with

V. V. Braguta, M. N. Chernodub, I. E. Kudrov, D. A. Sychev

[1] Joint Institute for Nuclear Research, Bogoliubov Laboratory of Theoretical Physics
roenko@theor.jinr.ru

The 40th International Symposium on Lattice Field Theory (LATTICE2023)
Fermilab, USA, 3 August 2023
The work was supported by RSF grant No. 23-10-00072.

Introduction

- In non-central heavy ion collisions creation of QGP with angular momentum is expected.

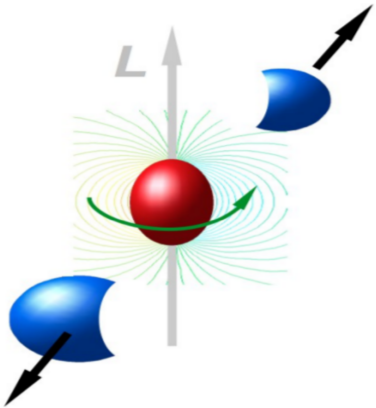

Introduction

- In non-central heavy ion collisions creation of QGP with angular momentum is expected.
- The rotation occurs with relativistic velocities.

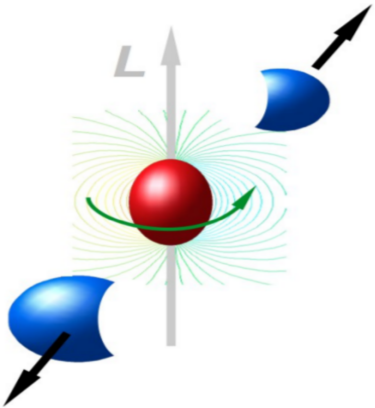

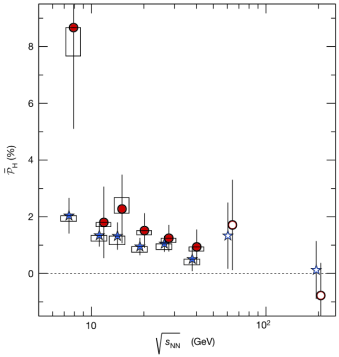

[L. Adamczyk et al. (STAR), Nature **548**, 62–65 (2017), arXiv:1701.06657 [nucl-ex]]

$\langle\omega\rangle \sim 6$ MeV ($\sqrt{s_{NN}}$-averaged)

Related papers and theoretical predictions

All* theoretical models assume that the system rotates like rigid body, $\Omega \neq 0$.

Properties of rotating QCD matter (mostly within NJL, focused on fermions):

- Z. Zhang, C. Shi, X.-T. He, X. Luo, and H.-S. Zong, Phys. Rev. D **102**, 114023 (2020), arXiv:2012.01017 [hep-ph]
- H. Zhang, D. Hou, and J. Liao, Chin. Phys. C **44**, 111001 (2020), arXiv:1812.11787 [hep-ph]
- X. Wang, M. Wei, Z. Li, and M. Huang, Phys. Rev. D **99**, 016018 (2019), arXiv:1808.01931 [hep-ph]
- M. Chernodub and S. Gongyo, JHEP **01**, 136 (2017), arXiv:1611.02598 [hep-th]
- ...
- Y. Jiang and J. Liao, Phys. Rev. Lett. **117**, 192302 (2016), arXiv:1606.03808 [hep-ph]

Rotation suppress the chiral condensate ($S = 0$), states with $S \neq 0$ are preferable.

$\Rightarrow$ Critical temperature of the chiral transition decreases due to the rotation.

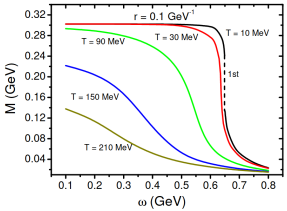

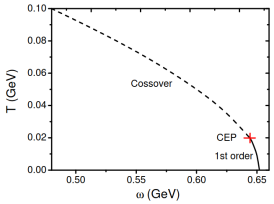

Related papers and theoretical predictions

Phase diagram of rotating QCD also studied within various other approaches:

- Holography: X. Chen, L. Zhang, D. Li, D. Hou, and M. Huang, JHEP **07**, 132 (2021), arXiv:2010.14478 [hep-ph], N. R. F. Braga, L. F. Faulhaber, and O. C. Junqueira, Phys. Rev. D **105**, 106003 (2022), arXiv:2201.05581 [hep-th], A. A. Golubtsova, E. Gourgoulhon, and M. K. Usova, Nucl. Phys. B **979**, 115786 (2022), arXiv:2107.11672 [hep-th], A. A. Golubtsova and N. S. Tsegelnik, Phys. Rev. D **107**, 106017 (2023), arXiv:2211.11722 [hep-th] Y.-Q. Zhao, S. He, D. Hou, L. Li, and Z. Li, JHEP **04**, 115 (2023), arXiv:2212.14662 [hep-ph], ...
- Compact QED in 2+1-D M. N. Chernodub, Phys. Rev. D **103**, 054027 (2021), arXiv:2012.04924 [hep-ph]
- HRG model: Y. Fujimoto, K. Fukushima, and Y. Hidaka, Phys. Lett. B **816**, 136184 (2021), arXiv:2101.09173 [hep-ph]
- Perturbative Polyakov loop potential in YM with Ω_I: S. Chen, K. Fukushima, and Y. Shimada, Phys. Rev. Lett. **129**, 242002 (2022), arXiv:2207.12665 [hep-ph]
- FRG: H.-L. Chen, Z.-B. Zhu, and X.-G. Huang, (2023), arXiv:2306.08362 [hep-ph]
- PNJL: F. Sun, K. Xu, and M. Huang, (2023), arXiv:2307.14402 [hep-ph]
- ...

$\Rightarrow$ The deconfinement critical temperature is predicted to decrease due to rotation.

Related papers and theoretical predictions

Our lattice results for gluodynamics is opposite: confinement critical temperature increases with rotation.

- V. V. Braguta, A. Y. Kotov, D. D. Kuznedelev, and A. A. Roenko, JETP Lett. **112**, 6–12 (2020)
- V. V. Braguta, A. Y. Kotov, D. D. Kuznedelev, and A. A. Roenko, Phys. Rev. D **103**, 094515 (2021), arXiv:2102.05084 [hep-lat]
- V. Braguta, A. Y. Kotov, D. Kuznedelev, and A. Roenko, PoS **LATTICE2021**, 125 (2022), arXiv:2110.12302 [hep-lat]

Related papers and theoretical predictions

Our lattice results for gluodynamics is opposite: confinement critical temperature increases with rotation.

- V. V. Braguta, A. Y. Kotov, D. D. Kuznedelev, and A. A. Roenko, JETP Lett. **112**, 6–12 (2020)
- V. V. Braguta, A. Y. Kotov, D. D. Kuznedelev, and A. A. Roenko, Phys. Rev. D **103**, 094515 (2021), arXiv:2102.05084 [hep-lat]
- V. Braguta, A. Y. Kotov, D. Kuznedelev, and A. Roenko, PoS **LATTICE2021**, 125 (2022), arXiv:2110.12302 [hep-lat]

Lattice results for QCD: the chiral and deconfinement critical temperatures both increase with rotation (decrease with imaginary rotation); fermions and gluons have opposite influence on T_c.

- V. V. Braguta, A. Kotov, A. Roenko, and D. Sychev, PoS **LATTICE2022**, 190 (2023), arXiv:2212.03224 [hep-lat]

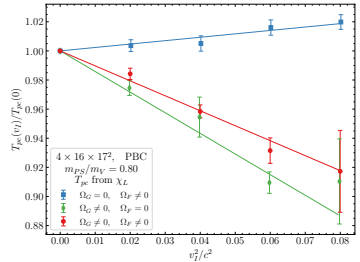

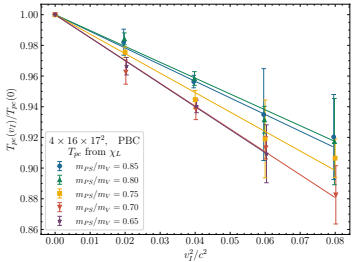

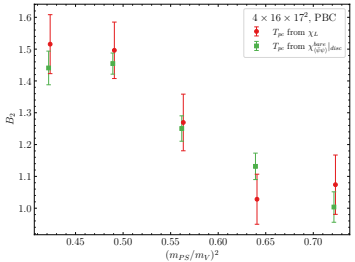

Related papers and theoretical predictions

Our lattice results for gluodynamics is opposite: confinement critical temperature increases with rotation.

- V. V. Braguta, A. Y. Kotov, D. D. Kuznedelev, and A. A. Roenko, JETP Lett. **112**, 6–12 (2020)
- V. V. Braguta, A. Y. Kotov, D. D. Kuznedelev, and A. A. Roenko, Phys. Rev. D **103**, 094515 (2021), arXiv:2102.05084 [hep-lat]
- V. Braguta, A. Y. Kotov, D. Kuznedelev, and A. Roenko, PoS **LATTICE2021**, 125 (2022), arXiv:2110.12302 [hep-lat]

Lattice results for QCD: the chiral and deconfinement critical temperatures both increase with rotation (decrease with imaginary rotation); fermions and gluons have opposite influence on T_c.

- V. V. Braguta, A. Kotov, A. Roenko, and D. Sychev, PoS **LATTICE2022**, 190 (2023), arXiv:2212.03224 [hep-lat]

Taking into account the contribution of rotating gluons to NJL model gives a similar prediction.

- Y. Jiang, Eur. Phys. J. C **82**, 949 (2022), arXiv:2108.09622 [hep-ph]

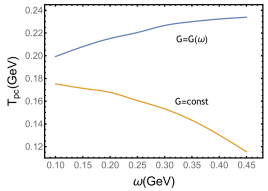

The running effective coupling $G(\omega)$ is introduced.

$\Rightarrow$ Critical temperature of the chiral transition increases due to the rotation.

Related papers and theoretical predictions

Our lattice results for gluodynamics is opposite: confinement critical temperature increases with rotation.

- V. V. Braguta, A. Y. Kotov, D. D. Kuznedelev, and A. A. Roenko, JETP Lett. **112**, 6–12 (2020)
- V. V. Braguta, A. Y. Kotov, D. D. Kuznedelev, and A. A. Roenko, Phys. Rev. D **103**, 094515 (2021), arXiv:2102.05084 [hep-lat]
- V. Braguta, A. Y. Kotov, D. Kuznedelev, and A. Roenko, PoS **LATTICE2021**, 125 (2022), arXiv:2110.12302 [hep-lat]

Lattice results for QCD: the chiral and deconfinement critical temperatures both increase with rotation (decrease with imaginary rotation); fermions and gluons have opposite influence on T_c.

- V. V. Braguta, A. Kotov, A. Roenko, and D. Sychev, PoS **LATTICE2022**, 190 (2023), arXiv:2212.03224 [hep-lat]

Taking into account the contribution of rotating gluons to NJL model gives a similar prediction.

- Y. Jiang, Eur. Phys. J. C **82**, 949 (2022), arXiv:2108.09622 [hep-ph]

Gluon contribution is crucial for rotating QCD!

Equation of State and Moment of Inertia

A mechanical response of a thermodynamic ansamble to rigid rotation $\boldsymbol{\Omega} = \Omega \boldsymbol{e}$ is described in terms of the total angular momentum $\boldsymbol{J}$. The energy in co-rotating reference frame is

$$E = E^{(lab)} - \boldsymbol{J} \cdot \boldsymbol{\Omega}\,, \qquad F = E - TS\,, \qquad dF = -SdT - \boldsymbol{J} \cdot d\boldsymbol{\Omega} + \dots\,,$$

The moment of inertia is a scalar quantity, $\boldsymbol{J} = I(T,\Omega)\boldsymbol{\Omega}$,

$$I(T,\Omega) = \frac{J(T,\Omega)}{\Omega} = -\frac{1}{\Omega}\left(\frac{\partial F}{\partial \Omega}\right)_T\,,$$

Equation of State and Moment of Inertia

A mechanical response of a thermodynamic ansamble to rigid rotation $\boldsymbol{\Omega} = \Omega \boldsymbol{e}$ is described in terms of the total angular momentum $\boldsymbol{J}$. The energy in co-rotating reference frame is

$$E = E^{(lab)} - \boldsymbol{J} \cdot \boldsymbol{\Omega}\,, \qquad F = E - TS\,, \qquad dF = -SdT - \boldsymbol{J} \cdot d\boldsymbol{\Omega} + \dots\,,$$

The moment of inertia is a scalar quantity, $\boldsymbol{J} = I(T,\Omega)\boldsymbol{\Omega}$,

$$I(T,\Omega) = \frac{J(T,\Omega)}{\Omega} = -\frac{1}{\Omega}\left(\frac{\partial F}{\partial \Omega}\right)_T\,,$$

For a classical system with characteristic radius R the moment of inertia is given by

$$I(T,\Omega) = \int_V d^3x\, x_\perp^2 \rho(T, x_\perp, \Omega) \simeq \alpha\, \rho_0(T) V R^2\,,$$

The free energy may be represented as a series in angular velocity (or linear velocity $v_R = \Omega R$)

$$F(T,V,\Omega) = F_0(T,V) - \frac{F_2(T,V)}{2}\Omega^2 + \mathcal{O}(\Omega^4) \equiv F_0(T,V)\left(1 + \frac{K_2}{2} v_R^2 + \mathcal{O}(v_R^4)\right)$$

where $F_2(T,V) = I(T,V,\Omega=0) \equiv -K_2 F_0 R^2$ (note, that $F_0 = -pV < 0$), and K_2 is dimensionless.

We study quenched QCD in the co-rotating reference frame (it rotates with angular velocity Ω around z-axis) $\rightarrow$ external gravitational field [A. Yamamoto and Y. Hirono, Phys. Rev. Lett. **111**, 081601 (2013), arXiv:1303.6292 [hep-lat]]

$$g^E_{\mu\nu} = \begin{pmatrix} 1 & 0 & 0 & x_2\Omega_I \\ 0 & 1 & 0 & -x_1\Omega_I \\ 0 & 0 & 1 & 0 \\ x_2\Omega_I & -x_1\Omega_I & 0 & 1 + x_\perp^2\Omega_I^2 \end{pmatrix}, \tag{1}$$

where $x_\perp^2 = x_1^2 + x_2^2$, and the angular velocity is put in the purely imaginary form $\Omega_I = -i\Omega$ to avoid the sign problem. The partition function is

$$Z = \int DA \, \exp\big(-S_G[A, \Omega]\big) \, . \tag{2}$$

The gluon action has the following form:

$$S = \frac{1}{4g_0^2}\int d^4x\,\sqrt{g_E}\,g_E^{\mu\nu}\,g_E^{\alpha\beta}F^a_{\mu\alpha}F^a_{\nu\beta} \equiv S_0 + S_1\Omega_I + S_2\frac{\Omega_I^2}{2}\,, \tag{3}$$

where

$$S_0 = \frac{1}{4g_0^2}\int d^4x F^a_{\mu\nu}F^a_{\mu\nu}\,, \tag{4}$$

$$S_1 = \frac{1}{g_0^2}\int d^4x\left[x_2F^a_{12}F^a_{24} + x_2F^a_{13}F^a_{34} - x_1F^a_{21}F^a_{14} - x_1F^a_{23}F^a_{34}\right], \tag{5}$$

$$S_2 = \frac{1}{g_0^2}\int d^4x\left[x_\perp^2(F^a_{12})^2 + x_2^2(F^a_{13})^2 + x_1^2(F^a_{23})^2 + 2x_1x_2F^a_{13}F^a_{32}\right], \tag{6}$$

The gluon action has the following form:

$$S = \frac{1}{4g_0^2}\int d^4x\,\sqrt{g_E}\,g_E^{\mu\nu}\,g_E^{\alpha\beta}F^a_{\mu\alpha}F^a_{\nu\beta} \equiv S_0 + S_1\Omega_I + S_2\frac{\Omega_I^2}{2}\,, \tag{3}$$

where

$$S_0 = \frac{1}{4g_0^2}\int d^4x F^a_{\mu\nu}F^a_{\mu\nu}\,, \tag{4}$$

$$S_1 = \frac{1}{g_0^2}\int d^4x\,[x_2F^a_{12}F^a_{24} + x_2F^a_{13}F^a_{34} - x_1F^a_{21}F^a_{14} - x_1F^a_{23}F^a_{34}]\,, \tag{5}$$

$$S_2 = \frac{1}{g_0^2}\int d^4x\big[x_\perp^2(F^a_{12})^2 + x_2^2(F^a_{13})^2 + x_1^2(F^a_{23})^2 + 2x_1x_2F^a_{13}F^a_{32}\big], \tag{6}$$

Sign problem

- The Euclidean action is complex-valued function with real rotation ($S_1 \neq 0$)!
- The Monte–Carlo simulations are conducted with imaginary angular velocity $\Omega_I = -i\Omega$.
- The results are analytically continued to the region of the real angular velocity ($\Omega_I^2 = -\Omega^2$, $v_I^2 = -v_R^2$).

- We use tree-level improved Symanzik gauge action (for S_0) and calculate free energy density $f = F/V$ using standard relations, which follows from $F/T = -\ln Z$,

$$\frac{f(T)}{T^4} = -N_t^4 \int_{\beta_0}^{\beta} d\beta' \Delta s(\beta') \,, \qquad \Delta s(\beta) = \langle s(\beta) \rangle_{T=0} - \langle s(\beta) \rangle_T \,,$$

where $\beta = 2N_c/g_0^2$ and $s = T/V \cdot S$ is the density of the lattice action S, and $\langle S \rangle = -\partial \ln Z / \partial \beta$.

- We use tree-level improved Symanzik gauge action (for S_0) and calculate free energy density $f = F/V$ using standard relations, which follows from $F/T = -\ln Z$,

$$\frac{f(T)}{T^4} = -N_t^4 \int_{\beta_0}^{\beta} d\beta' \Delta s(\beta')\,, \qquad \Delta s(\beta) = \langle s(\beta)\rangle_{T=0} - \langle s(\beta)\rangle_T\,,$$

  where $\beta = 2N_c/g_0^2$ and $s = T/V \cdot S$ is the density of the lattice action S, and $\langle S\rangle = -\partial \ln Z/\partial\beta$.
- The free energy density also relates to the scale (trace) anomaly

$$\frac{f(T)}{T^4} = -\int_0^T \frac{dT'}{T'} \frac{\langle T^\mu_{\ \mu}\rangle(T')}{T'^4}\,, \qquad \frac{\langle T^\mu_{\ \mu}\rangle}{T^4} = -N_t^4 a \frac{d\beta}{da}\Delta s = N_t^4 T \frac{d\beta}{dT}\Delta s\,. \tag{7}$$

- Therefore, the moment of inertia is connected to the rotational response of the scale anomaly:

$$I(T) = -VT^4 \int_0^T \frac{dT'}{T'} \frac{\langle T^\mu_{\ \mu}\rangle^{(2)}(T')}{T'^4}\,, \qquad \langle T^\mu_{\ \mu}\rangle^{(2)}(T) = \left[\frac{\partial^2}{\partial\Omega_I^2}\langle T^\mu_{\ \mu}\rangle(T,\Omega_I)\right]\Bigg|_{\Omega_I=0}\,. \tag{8}$$

Results of lattice simulations with non-zero imaginary angular velocity

- $N_t \times 40 \times 41^2$ lattices with $N_t = 5, 6, 7, 8$;
- $N_t^{(T=0)} = 40$ for $T = 0$ subtraction;
- $v_I^2 \ll 1$, where $v_I = \Omega_I R$, $R = a(N_s - 1)/2$.

Results of lattice simulations with non-zero imaginary angular velocity

- $N_t \times 40 \times 41^2$ lattices with $N_t = 5, 6, 7, 8$;
- $N_t^{(T=0)} = 40$ for $T = 0$ subtraction;
- $v_I^2 \ll 1$, where $v_I = \Omega_I R$, $R = a(N_s - 1)/2$.

- The critical temperature decreases with the imaginary angular velocity.

- Fit by the quadratic function (note $f_0 =< 0$):

$$f(T, v_I) = f_0(T)\Big(1 - \frac{1}{2}K_2(T)v_I^2\Big).$$

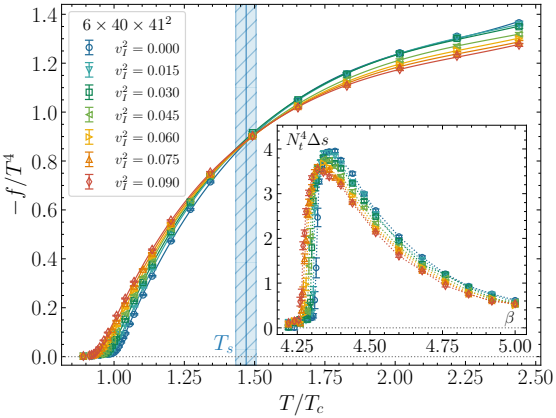

[V. V. Braguta, M. N. Chernodub, A. A. Roenko, and D. A. Sychev, (2023), arXiv:2303.03147 [hep-lat]]

Results of lattice simulations with non-zero imaginary angular velocity

- The moment of inertia of gluon plasma

$$I(T)|_{\Omega=0} = -K_2 F_0 R^2 \,,$$

becomes zero at "supervortical" temperature

$$T_s = 1.50(10) T_c.$$

and it is negative for $T < T_s$.

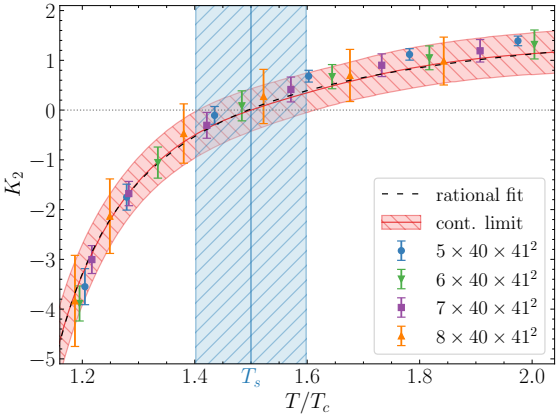

[V. V. Braguta, M. N. Chernodub, A. A. Roenko, and D. A. Sychev, (2023), arXiv:2303.03147 [hep-lat]]

Results of lattice simulations with non-zero imaginary angular velocity

- The moment of inertia of gluon plasma

$$I(T)|_{\Omega=0} = -K_2 F_0 R^2 \,,$$

becomes zero at "supervortical" temperature

$$T_s = 1.50(10) T_c.$$

and it is negative for $T < T_s$.

- K_2 can be reproduced by a rational function

$$K_2^{(\mathrm{fit})}(T) = K_2^{(\infty)} - \frac{c}{T/T_c - 1} \,,$$

where $K_2^{(\infty)} = 2.23(39)$ and $c = 1.11(20)$.

- The result for the system with OBC is

$$T_s = 1.53(15) T_c$$

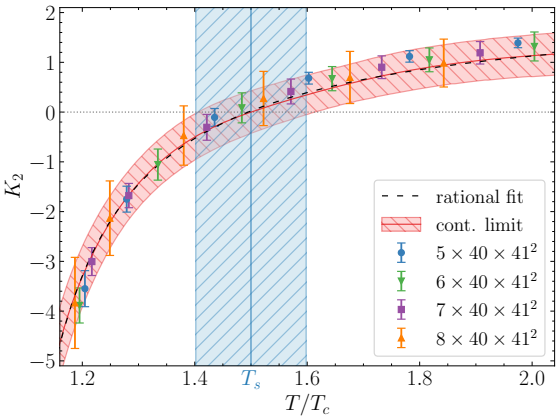

[V. V. Braguta, M. N. Chernodub, A. A. Roenko, and D. A. Sychev, (2023), arXiv:2303.03147 [hep-lat]]

Condition of thermodynamic stability

For a system in a stable equilibrium at a given T and $\mathbf{\Omega}$, any deviation from the equilibrium should obey the following condition [L. D. Landau and E. M. Lifshitz, 3rd ed. (Butterworth-Heinemann, Oxford, England, Aug. 1996)]:

$$\delta E - T\delta S - \mathbf{\Omega}\delta \boldsymbol{J} > 0\,, \tag{9}$$

which implies that all eigenvalues of the inverse Weinhold metric, defined in the thermodynamic space [F. Weinhold, The Journal of Chemical Physics **63**, 2479–2483 (1975)],

$$g^{(W),\mu\nu} = -\frac{\partial^2 f(T,\mathbf{\Omega})}{\partial X_\mu \partial X_\nu}\,, \qquad\qquad X_\mu = (T, \Omega_i)\,, \tag{10}$$

must be positively defined. It is equivalent to the requirements

$$C_J = T\left(\partial S/\partial T\right)_J > 0\,, \qquad\qquad \mathrm{spec}(I^{ij}) > 0\,, \tag{11}$$

where $I^{ij} \equiv I^{ji} = \left(\partial J^i/\partial \Omega_j\right)_T$. In terms of the coefficient K_2, the thermodynamic stability thus requires:

$$\boxed{K_2(T) > 0 \qquad \text{(thermodynamic stability)},}$$

which is violated below the supervortical temperature, $T < T_s$. This instability has a thermodynamic origin. Similar instabilities occur in curved gravitational backgrounds of rotating Kerr and Myers-Perry black holes.

Taking the derivative at $\Omega = 0$, we obtain:

$$I = F_2 = T\frac{\partial^2 \log Z}{\partial \Omega^2}\bigg|_{\Omega=0} = T\big(\langle\langle S_1^2\rangle\rangle_T + \langle\langle S_2\rangle\rangle_T\big)\,,$$

where $\langle\langle \mathcal{O}\rangle\rangle_T = \langle\mathcal{O}\rangle_T - \langle\mathcal{O}\rangle_{T=0}$ corresponds to the thermal contribution to $\langle\mathcal{O}\rangle$.

$$f_2 = F_2/V,\ F_2 \sim \rho_0 V R^2 \quad \Rightarrow \quad f_2/(T^4 L_s^2) \sim \rho_0/T^4$$

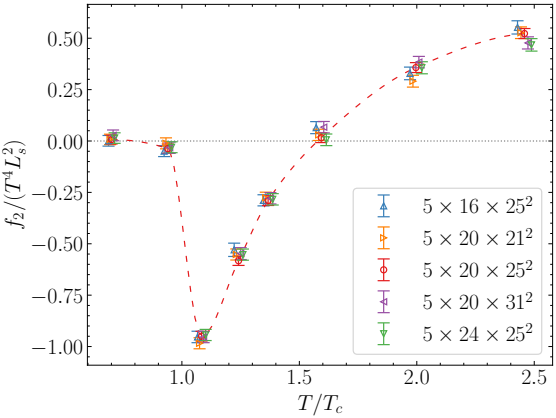

[V. V. Braguta, I. E. Kudrov, A. A. Roenko, D. A. Sychev, and M. N. Chernodub, JETP Lett. **117**, 639–644 (2023)]

Taking the derivative at $\Omega = 0$, we obtain:

$$I = F_2 = T\frac{\partial^2 \log Z}{\partial \Omega^2}\bigg|_{\Omega=0} = T\big(\langle\langle S_1^2\rangle\rangle_T + \langle\langle S_2\rangle\rangle_T\big)\,,$$

where $\langle\langle\mathcal{O}\rangle\rangle_T = \langle\mathcal{O}\rangle_T - \langle\mathcal{O}\rangle_{T=0}$ corresponds to the thermal contribution to $\langle\mathcal{O}\rangle$.

$$f_2 = F_2/V,\ F_2 \sim \rho_0 V R^2 \quad \Rightarrow \quad f_2/(T^4 L_s^2) \sim \rho_0/T^4$$

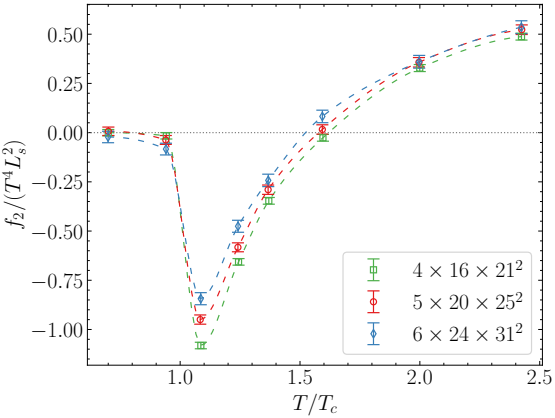

[V. V. Braguta, I. E. Kudrov, A. A. Roenko, D. A. Sychev, and M. N. Chernodub, JETP Lett. **117**, 639–644 (2023)]

Taking the derivative at $\Omega = 0$, we obtain:

$$I = F_2 = T\frac{\partial^2 \log Z}{\partial \Omega^2}\bigg|_{\Omega=0} = T\big(\langle\langle S_1^2\rangle\rangle_T + \langle\langle S_2\rangle\rangle_T\big)\,,$$

where $\langle\langle\mathcal{O}\rangle\rangle_T = \langle\mathcal{O}\rangle_T - \langle\mathcal{O}\rangle_{T=0}$ corresponds to the thermal contribution to $\langle\mathcal{O}\rangle$.

$$K_2 = -4F_2/(F_0 L_s^2) \sim \rho_0/f_0$$

At supervortical temperature $K_2(T_s) = 0$

$$T_s \simeq 1.5 T_c$$

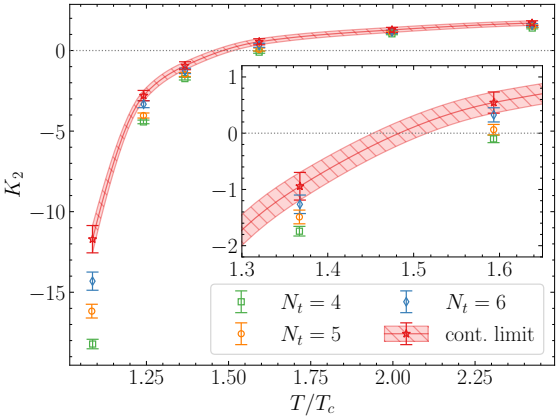

[V. V. Braguta, I. E. Kudrov, A. A. Roenko, D. A. Sychev, and M. N. Chernodub, JETP Lett. **117**, 639–644 (2023)]

Using the exact forms of S_1, S_2, we get

$$I = I_{fluct} + I_{cond}$$

where ($\langle J^3 \rangle = 0$ for any T) and

$$I_{\text{fluct}} = \frac{1}{T}\Big(\langle\langle (J^3)^2 \rangle\rangle_T - \langle\langle J^3 \rangle\rangle_T^2\Big) \geq 0,$$

$$I_{\text{cond}} = \frac{1}{3}\int_V d^3x\, x_\perp^2 \langle\langle (F_{ij}^a)^2 \rangle\rangle_T = \frac{\alpha}{3} V R^2 \langle\langle (F_{ij}^a)^2 \rangle\rangle_T .$$

J^3 is the total angular momentum of gluon field.

- Mass density $\rho_0(T) \leftrightarrow \langle\langle (F_{ij}^a)^2 \rangle\rangle_T / 3$.

Using the exact forms of S_1, S_2, we get

$$I = I_{fluct} + I_{cond}$$

where ($\langle J^3 \rangle = 0$ for any T) and

$$I_{\rm fluct} = \frac{1}{T}\Big(\langle\langle (J^3)^2 \rangle\rangle_T - \langle\langle J^3 \rangle\rangle_T^2 \Big) \geq 0,$$

$$I_{\rm cond} = \frac{1}{3}\int_V d^3x\, x_\perp^2 \langle\langle (F_{ij}^a)^2 \rangle\rangle_T = \frac{\alpha}{3} V R^2 \langle\langle (F_{ij}^a)^2 \rangle\rangle_T \,.$$

J^3 is the total angular momentum of gluon field.

- Mass density $\rho_0(T) \leftrightarrow \langle\langle (F_{ij}^a)^2 \rangle\rangle_T/3$.
- Magnetic gluon condensate reverse its sign at $T \sim 2T_c$. $\Rightarrow T_s < 2T_c$.

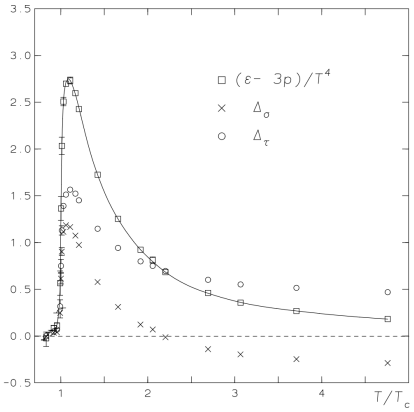

$$\Delta_\sigma \propto -\langle\langle (F_{ij}^a)^2 \rangle\rangle_T$$

[G. Boyd et al., Nucl. Phys. B **469**, 419–444 (1996), arXiv:hep-lat/9602007]

Using the exact forms of S_1, S_2, we get

$$I = I_{fluct} + I_{cond}$$

where ($\langle J^3 \rangle = 0$ for any T) and

$$I_{\text{fluct}} = \frac{1}{T}\Big(\langle\langle (J^3)^2 \rangle\rangle_T - \langle\langle J^3 \rangle\rangle_T^2\Big) \geq 0,$$

$$I_{\text{cond}} = \frac{1}{3}\int_V d^3x\, x_\perp^2 \langle\langle (F_{ij}^a)^2 \rangle\rangle_T = \frac{\alpha}{3} V R^2 \langle\langle (F_{ij}^a)^2 \rangle\rangle_T .$$

J^3 is the total angular momentum of gluon field.

- Mass density $\rho_0(T) \leftrightarrow \langle\langle (F_{ij}^a)^2 \rangle\rangle_T/3$.
- Magnetic gluon condensate reverse its sign at $T \sim 2T_c$. $\Rightarrow T_s < 2T_c$.
- In QCD only fermionic contribution to J^3 will be added.

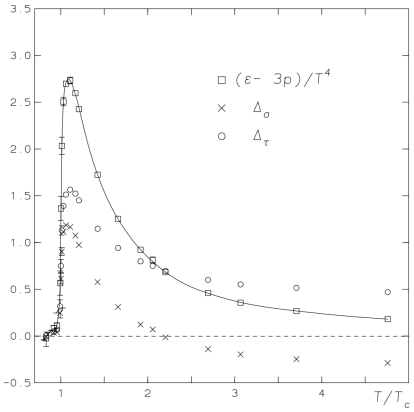

$$\Delta_\sigma \propto -\langle\langle (F_{ij}^a)^2 \rangle\rangle_T$$

[G. Boyd et al., Nucl. Phys. B **469**, 419–444 (1996), arXiv:hep-lat/9602007]

Conclusions

- We calculate the isothermal moment of inertia of *rigidly* rotating gluon plasma within lattice simulations using both analytic continuation ($f(T,\Omega_I)$) and derivative ($\partial^2 F/\partial\Omega^2\big|_{\Omega=0}$) methods; the results are in agreement.
- The moment of inertia unexpectedly takes a negative value below the "supervortical temperature" $T_s = 1.50(10)T_c$, vanishes at $T = T_s$, and becomes a positive quantity at higher temperatures.
- The negative moment of inertia indicates a thermodynamic instability of rigid rotation for $T < T_s$. We found the first lattice evidence of this instability in rotating QCD.
- The *rigid* rotation of quark-gluon plasma also should be unstable in a region near T_c due to the same reasons.
- The discrepancy between numerical (lattice) and various theoretical predictions may originate from scale anomaly, which should be taken into account appropriately. The magnetic gluon condensate plays the crucial role in rotating plasma.

See the details in:

- V. V. Braguta, M. N. Chernodub, A. A. Roenko, and D. A. Sychev, (2023), arXiv:2303.03147 [hep-lat]
- V. V. Braguta, I. E. Kudrov, A. A. Roenko, D. A. Sychev, and M. N. Chernodub, JETP Lett. **117**, 639–644 (2023)

Thank you for your attention!

Gluon lattice action

The (improved) lattice gluon action can be written as

$$S_G = \beta \sum_x \Big((c_0 + r^2\Omega_I^2) W_{xy}^{1\times1} + (c_0 + y^2\Omega_I^2) W_{xz}^{1\times1} + (c_0 + x^2\Omega_I^2) W_{yz}^{1\times1} + \\ + c_0 \big(W_{x\tau}^{1\times1} + W_{y\tau}^{1\times1} + W_{z\tau}^{1\times1} \big) + y\Omega_I \big(W_{xy\tau}^{1\times1\times1} + W_{xz\tau}^{1\times1\times1} \big) - \\ - x\Omega_I \big(W_{yx\tau}^{1\times1\times1} + W_{yz\tau}^{1\times1\times1} \big) + xy\Omega_I^2 W_{xzy}^{1\times1\times1} + \sum_{\mu\neq\nu} c_1 W_{\mu\nu}^{1\times2} \Big) , \quad (12)$$

with $\beta = 6/g^2$, and $c_0 = 1 - 8c_1$, where $c_1 = -1/12$ and

$$W_{\mu\nu}^{1\times1}(x) = 1 - \frac{1}{3}\mathrm{Re\ Tr}\ \bar{U}_{\mu\nu}(x) , \quad (13)$$

$$W_{\mu\nu}^{1\times2}(x) = 1 - \frac{1}{3}\mathrm{Re\ Tr}\ R_{\mu\nu}(x) , \quad (14)$$

$$W_{\mu\nu\rho}^{1\times1\times1}(x) = -\frac{1}{3}\mathrm{Re\ Tr}\ \bar{V}_{\mu\nu\rho}(x) , \quad (15)$$

$\bar{U}_{\mu\nu}$ denotes clover-type average of 4 plaquettes,

$R_{\mu\nu}$ is a rectangular loop,

$\bar{V}_{\mu\nu\rho}$ is asymmetric chair-type average of 8 chairs.

$$\int d^4x\sqrt{g_E}\,(\dots) = \int_0^{1/T} dx_0\sqrt{g_{44}}\int d^3x\sqrt{\gamma_E}\,(\dots) = \int_0^{1/T} dx_0 \int d^3x\sqrt{g_E}\,(\dots)$$

- Interpretation: Tolman-Ehrenfest effect. In gravitational field the temperature isn't a constant in space at thermal equilibrium:
$$T(r)\sqrt{g_{00}} = const\,,$$
- For the (real) rotation one has
$$T(r)\sqrt{1-r^2\Omega^2} = const \equiv T\,,$$
- One could expect, that the rotation effectively warm up the periphery of the modeling volume
$$T(r) > T(r=0),$$
and as a result, from kinematics, the critical temperature should decreases.
- Our results show that the behavior of the (pseudo-)critical temperatures is more complicated. It also may be caused by instability.

Rotating gluodynamics: OBC, Polyakov loop distribution

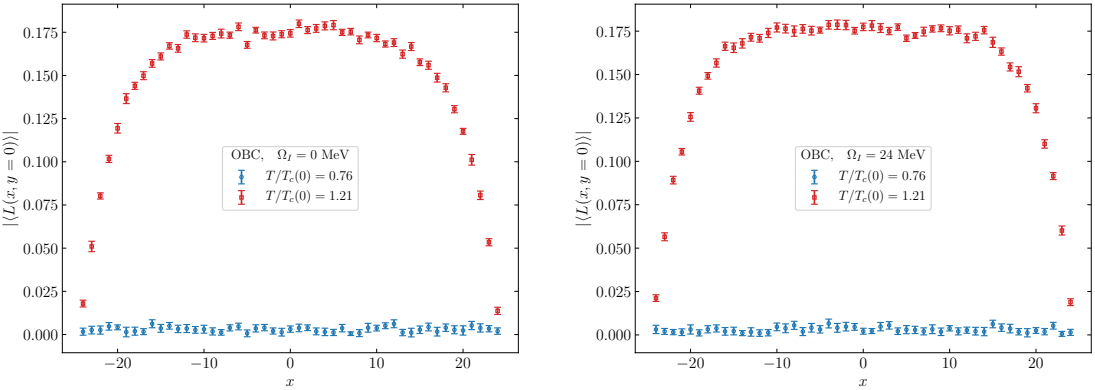

Figure: The local Polyakov loop $|\langle L(x, y)\rangle|$ as a function of coordinate for OBC and $\Omega_I = 0$ MeV (left), $\Omega_I = 24$ MeV (right). Points with $x \neq 0, y = 0$ from the lattice $8 \times 24 \times 49^2$ are shown.

- In deconfinement phase the boundary is screened.

Rotating gluodynamics: PBC, Polyakov loop distribution

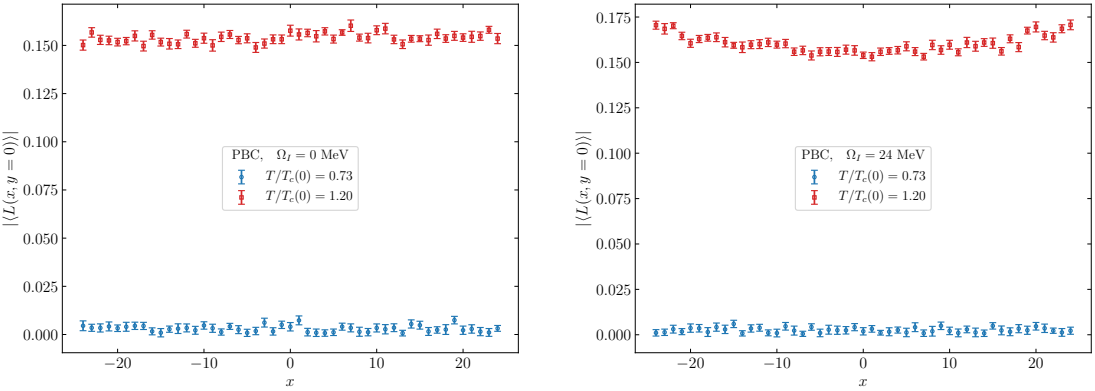

Figure: The local Polyakov loop $|\langle L(x, y)\rangle|$ as a function of coordinate for OBC and $\Omega_I = 0$ MeV (left), $\Omega_I = 24$ MeV (right). Points with $x \neq 0, y = 0$ from the lattice $8 \times 24 \times 49^2$ are shown.

- The local Polyakov loop demonstrates weak dependence on the coordinate in the deconfinement phase.

Rotating gluodynamics: DBC, Polyakov loop distribution

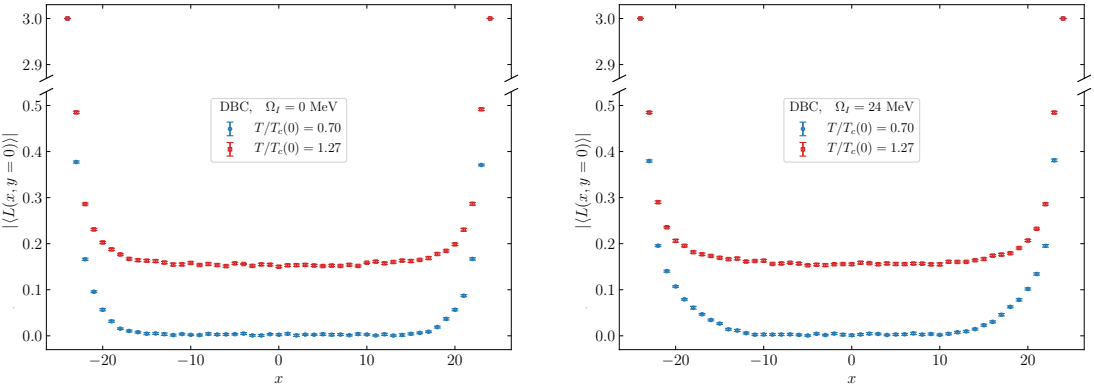

Figure: The local Polyakov loop $|\langle L(x, y)\rangle|$ as a function of coordinate for OBC and $\Omega_I = 0$ MeV (left), $\Omega_I = 24$ MeV (right). Points with $x \neq 0, y = 0$ from the lattice $8 \times 24 \times 49^2$ are shown.

- The boundary is screened.